JOURNAL OF MATERIALS SCIENCE **40** (2005) 3403 – 3407

A hybrid replication technique for the analysis of precipitate-boundary interactions in Ni-based superalloys

KAI SONG, MARK AINDOW*
Department of Materials Science and Engineering, Institute of Materials Science, University of Connecticut, Unit 3136, 97 North Eagleville Road, Storrs, CT 06269-3136, USA

A hybrid replication technique is described for complex alloy systems whereby the surface is etched to reveal the microstructure of the metallic phases prior to producing an extraction replica. By applying this approach to the Ni-based superalloy IN100, it has been shown that the inert carbide and boride particles can be extracted for analysis in the TEM whilst retaining information about their location with respect to the metallic phases in the alloy. This approach is particularly useful for studying the effects of inert particles on microstructural evolution, such as pinning effects during grain growth. © *2005 Springer Science + Business Media, Inc.*

1. Introduction

In the infancy of TEM work on metallic systems, carbon replication was one of the most common approaches to specimen preparation; but it is now used only very infrequently. The use of surface replicas in TEM has been superceded almost completely by high-resolution secondary electron imaging in the SEM. Similarly, the use of extraction replicas for the analysis of small second-phase particles [1–3] has declined due to recent advances in TEM instrumentation. In particular, the advent of field-emission-gun electron sources, low spherical-aberration-coefficient objective lenses, and advanced spectrometers now enables the morphology, structure and chemistry of particles in most alloys to be analyzed without the need for extraction.

There are, however, certain engineering alloys in which the microstructures are so complex, and/or the volume fractions of the particles are so low, that extraction replication can still be extremely helpful. Perhaps the best examples are steels or other ferrous alloys, and Ni-based superalloys. Commercial superalloys contain a variety of different precipitates in a face-centered cubic γ matrix. The majority of these correspond to the $L1_2$ (Ni_3Al) γ' phase, but inert precipitates like carbides and borides are often present as minority constituents (<1% by volume). These inert particles can have a profound influence on the microstructural stability and high-temperature mechanical properties because of the way in which they interact with the grain boundaries [4]. Although extraction replication can be a useful way to prepare samples in which these particles can be studied readily (e.g. [5, 6]), the main drawback is that they appear upon an almost featureless carbon support film, and hence the relationship of these particles to their microstructural environment is lost. This issue is particularly important in studies of grain boundary pinning wherein one would ideally wish to know which of the particles on an extraction replica corresponded to pinning sites in a given microstructural condition.

In our work we have studied pinning phenomena in the Ni-based superalloy IN100 and related alloys: the details of these studies will be published elsewhere. In this paper we describe a hybrid replication technique, developed during the course of these studies, in which the sample surface is etched carefully to reveal both the particles and other microstructural features such as grain boundaries before coating with carbon. The resultant replica not only extracts the inert particles but also reveals clearly the microstructure of the metal between them.

2. Materials and methods

All of the experimental images presented in this paper were obtained from powder-processed IN100. A typical composition for this alloy is: Ni-18.5Co-12.4Cr-5.0Al-4.3Ti-3.2Mo-0.8V-0.07Zr-0.07C-0.02B (all in weight %). The samples were subjected to a standard heat-treatment sequence consisting of a sub-solvus (1150 °C) solution treatment, followed by a two-step aging that involved holding at 980 °C and 730 °C, respectively. This process cycle results in a fairly complex microstructure that consists of a fine-grained γ matrix with three sizes of embedded γ' precipitates, usually designated primary, secondary and tertiary γ' [6]

*Author to whom all correspondence should be addressed.

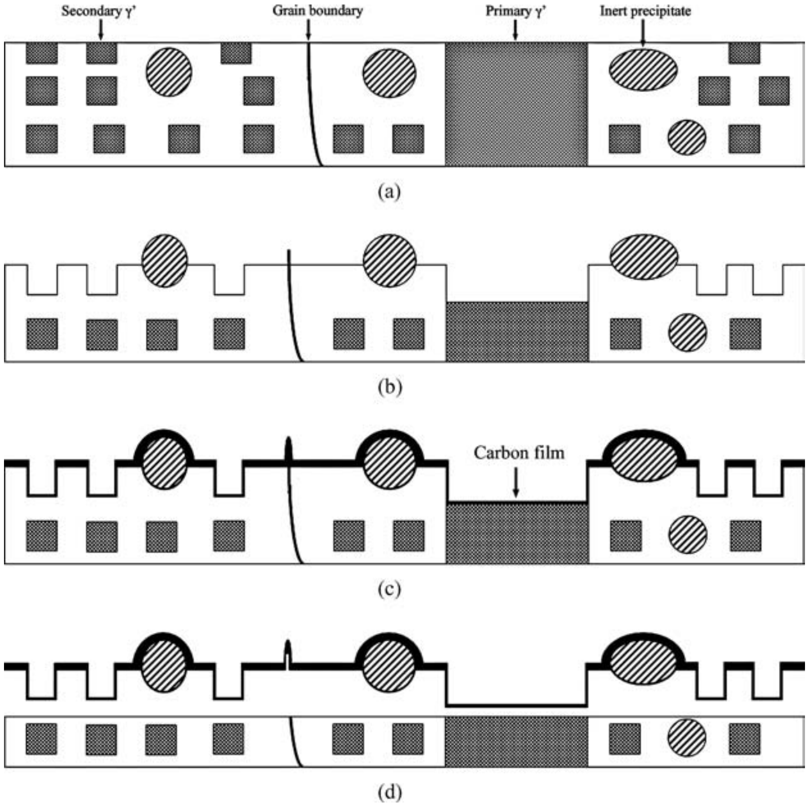

Figure 1 Schematic diagram of the main steps in the hybrid replication process: (a) featureless surface formed by polishing; (b) surface topography revealed by etching with Kalling's solution; (c) coating of the surface with C; (d) release of the replica during electro-etching.

plus transition metal carbides and borides. Grain growth phenomena were studied in these samples by holding for various times at temperatures between 1100 °C and 1250 °C.

The various stages in the preparation of the hybrid replicas are shown schematically in Fig. 1. Metallurgical sections cut from the alloy were ground mechanically to 1200 grit and then electro-polished to remove the surface damage layer. This was achieved by suspending the sample from a Pt wire in a solution of 10% HCl, 89% Methanol and 1% Citric acid held at a temperature of −45 °C, and applying a potential of 25V DC between this and a Ta foil cathode. This produced a featureless mirror-finish on the sample surface (Fig. 1a).

Immediately after the electro-polish, the sample was immersed in water-less Kalling's solution (40 ml HCl, 40 ml Ethanol and 2 g Cupric Chloride) at room temperature for 5 min. This procedure etched the γ phase lightly, and the γ' to a much greater extent, but did not affect the inert particles or the grain boundaries; thus, these latter features formed protrusions on the sample surface (Fig. 1b). To avoid over-sampling of the inert particles, the sample was oriented with the polished surface vertical during the etching; and was then rinsed thoroughly in ethanol to remove loose particulates.

The specimen surface was then replicated by evaporating ≈30 nm of carbon onto the etched sample (Fig. 1c) from a source inclined to the sample surface normal by ≈10 °. The carbon replicas were released by electro-etching using the same electrolyte as for the initial electropolish, but at 0–10°C under current control at a density of 0.03–0.05 A/cm^2. This process gave a further, more rapid dissolution of both γ and γ' phases, enabling the fine inert particles to be extracted without difficulty (Fig. 1d). To ease the subsequent lifting of the replicas, the specimen surface was scored into small (≈2 × 2 mm) squares prior to electro-etching. Typical electro-etch times required for release of the replicas ranged from 1 to 5 min. The brevity of this process reduces the contamination to a minimum and ensures that the extracted material in the replica reproduces the distribution in the sample more faithfully.

The replicas were lifted from specimen surface by sliding the specimen gently into a water bath. By adjusting the inclination of the sample, and the speed at which it was submerged, it was possible to transfer the released replicas onto the surface of the bath. The replicas were left in the bath for several minutes to wash any residual electrolyte from the surface, and were then lifted onto 300 mesh Cu support grids. The supported replicas were examined in a Philips EM420 TEM and a JEOL 2010 FasTEM, operating at 100 and 200kV, respectively. The latter instrument is equipped with an EDAX Phoenix atmospheric thin window energy-dispersive X-ray spectrometer (EDXS). Bright field images were obtained from the replicas with the objective lens underfocused somewhat to enhance the contrast from the thin C film.

3. Examples of data from the replicas

A series of TEM micrographs that show the main features of the replicas is presented in Fig. 2a. These

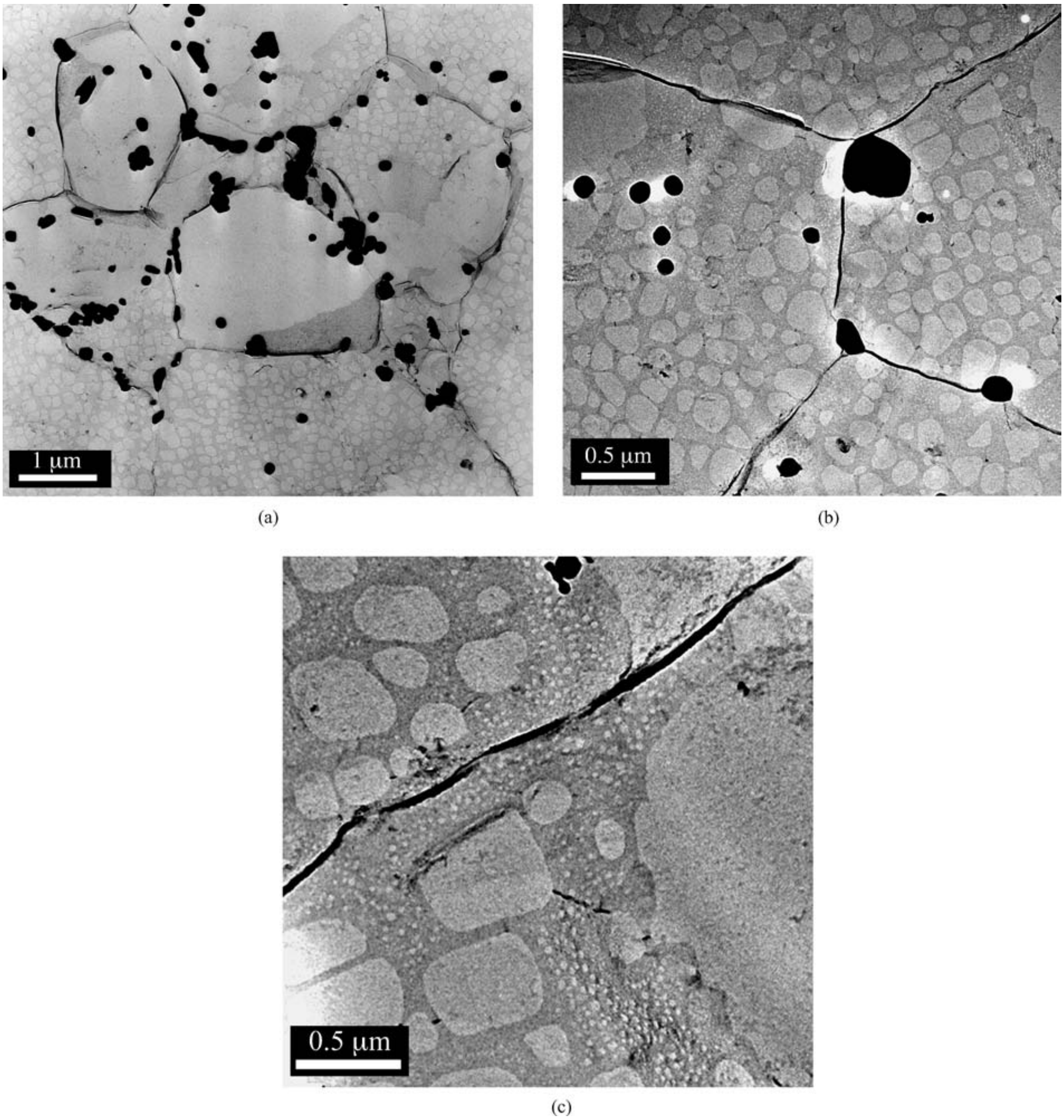

Figure 2 Bright field TEM micrographs showing the replication of surface topography in the C: (a) overall view showing the location of primary γ' phase (bright), γ grains (mottled) and the grain/interphase boundaries (dark lines); (b) enlarged view showing the secondary γ' phase within the γ grains; (c) detail of the region shown in (b) which reveals the tertiary γ' phase in the γ channels between the secondary γ' precipitates.

replicas were obtained from the starting microstructure in IN100, i.e. prior to grain growth studies. The region shown in Fig. 2a is from an area which contained grains of the γ matrix and large primary γ' grains >1 μm in diameter. Although the two types of grains are of similar sizes, the γ matrix can be distinguished easily because the C film is thicker in these regions and exhibits a "mottled" contrast. The C film is thinner at the locations of the primary γ' grains because the Kalling's solution attacks the γ' phase preferentially. Thus, the surfaces of the cavities caused by the etching out of the primary γ' grains are "shadowed" leading to thinner films in most locations. This shadowing effect also leads to the accumulation of carbon at the protruding grain boundaries on the etched surface, and therefore the γ/γ and γ/γ' boundaries are delineated clearly in the replicas. Higher magnification images such as Fig. 2b show that the "mottled" contrast in the C film at the positions of the γ matrix grains corresponds to the replication of the secondary or "aging" γ'. These form as coherent precipitates within the γ grains and develop into cuboidal semi-coherent particles 100–300 nm across. Images obtained at even higher magnifications (e.g. Fig. 2c) show that the finest tertiary γ' precipitates are also replicated. These spheroidal coherent particles precipitate within the γ channels between the secondary γ' precipitates and have diameters of <15 nm. We note that the dimensions of the microstructural features measured from the replicas correspond closely to those obtained using other techniques [6].

Because the carbide and boride particles are not affected significantly by the chemical reagents used in

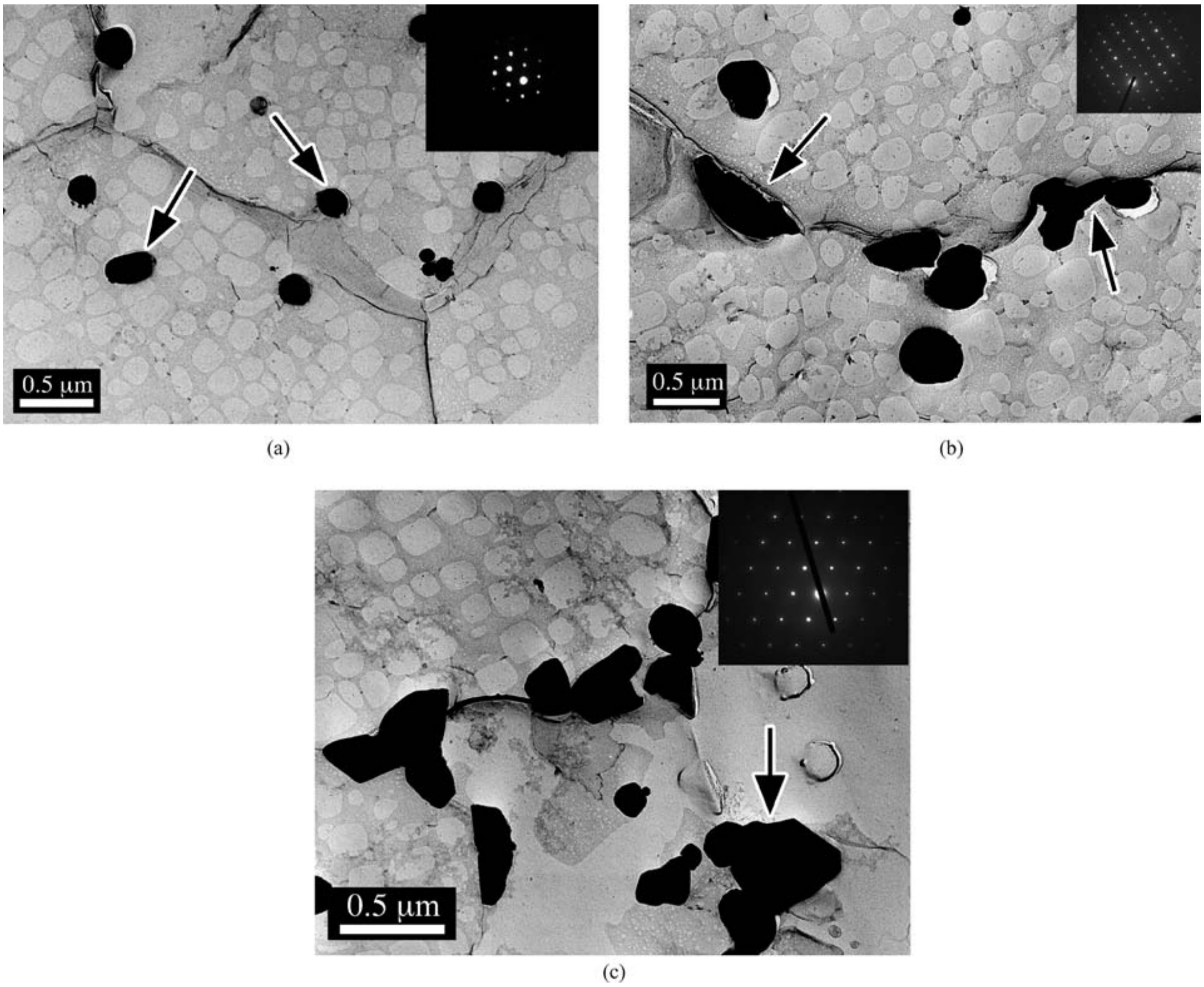

Figure 3 Bright field TEM micrographs with inset SADPs showing examples of the three types of inert particles observed in the alloy: (a) MC-type; (b) $M_{23}C_6$-type; (c) M_3B_2-type.

the preparation, they are much thicker than the C film and appear black in the images. Examples of the three main types of extracted particles are shown in Figs. 3a–c with insets corresponding to typical selected-area electron diffraction patterns. There are two types of carbides present: MC-type with the cubic NaCl structure, and $M_{23}C_6$-type with the cubic $Cr_{23}C_6$ structure. There are also M_3B_2-type borides with the tetragonal U_3Si_2 structure. The MC carbides are distributed homogeneously throughout the microstructure, are equi-axed with diameters of ≈200 nm (Fig. 3a), and are Ti-rich as revealed by EDXS. The $M_{23}C_6$-type and M_3B_2-type particles are coarser (up to 1 μm), have more irregular morphologies, and tend to be located at the γ/γ and γ/γ' boundaries (Figs 3b and c). The $M_{23}C_6$-type particles are Cr-rich whereas the M_3B_2-type particles are enriched in both Mo and Cr.

Subsequent heat-treatment of the IN100 resulted in an initial rapid increase in grain size, followed by stagnation after a few hours. Such behavior is characteristic of Zener pinning by particles [7]. This process results in the cessation of grain growth once a limiting grain size has been reached: the value of the limiting grain size depends upon both the volume fraction of the particles and their size. The pinning phenomena in IN100 are complex and include contributions from both the primary γ' grains and the inert particles (carbides and borides). For samples in which the grains had grown to the limiting size, examination of the replicas revealed that, in each case, the MC-type carbides play a key role in pinning the grain boundaries. Three examples of images obtained from such replicas are presented in Fig. 4. Fig. 4a is from a boundary region that is pinned by four separate MC particles: the overall curvature indicates the direction in which the boundary had migrated, and the local curvature reveals the retarding effect of the carbide particle in accordance with the classical "dimple model' [8]. The region shown in Fig. 4b contains a small single grain pinned by several MC carbides. This emphasizes the point that whilst the average grain size increases to a limiting value during heat-treatment, the sizes of the individual grains depend on the local particle distribution in such microstructures. In the final example (Fig. 4c), there are two MC particles, one on either side of the boundary. From the local curvatures, it is clear that both of the particles are influencing the boundary migration. This is known as the Louat effect [9], wherein particles behind the boundary retard its motion but particles ahead of it enhance the motion at this point.

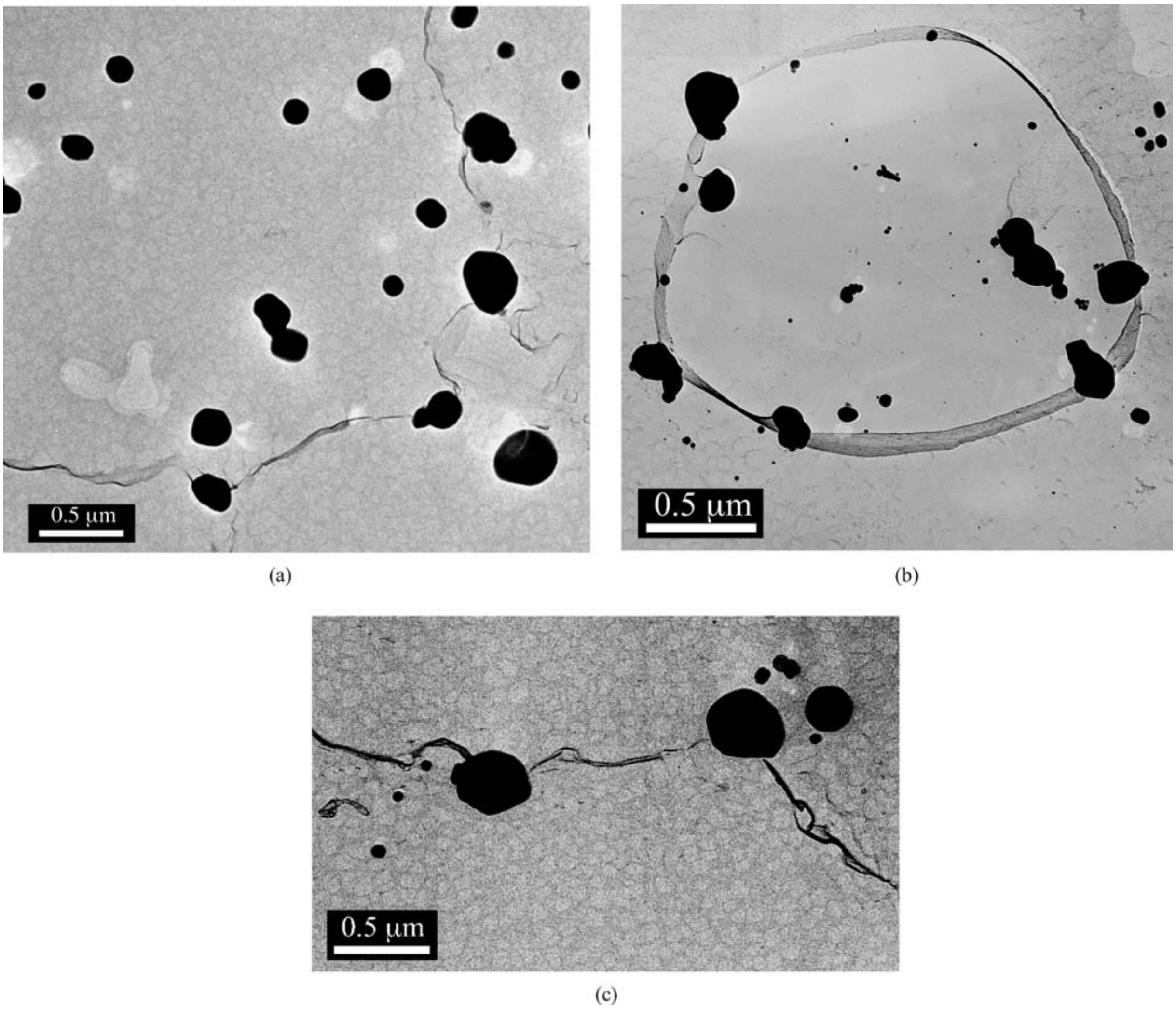

Figure 4 Bright field TEM micrographs showing examples of boundary/particle interactions. The pinning particles at the boundary are MC-type in each case.

4. Conclusions

It has been shown that by applying a suitable etch to the surface of metallographic samples of IN100, it is possible to produce hybrid carbon replicas that both extract the inert carbide and boride particles and reveal the microstructure of the metallic phases in which they form. These replicas offer the same advantages as conventional extraction replicas in analyses of the morphologies, crystal structures and compositions of the inert particles. They are, however, much more informative in studies of the role which such particles play in microstructural development. Perhaps the best example of this is in studies of boundary pinning during grain growth. Although the reagents and experimental conditions described in this paper are only appropriate for IN100 and closely related Ni-based superalloys, this general approach could be adapted for use with other complex alloy systems.

Acknowledgements

The authors are grateful to the late Professor Martin J. Blackburn who suggested that carbon replication could be adapted for the study of particle/boundary interactions in such alloys. This work was supported by DARPA/USAF under Contract No F33615-00-2-5216 with Dr. R. Dutton as technical monitor. The authors would like to thank Dr. Michael F. Savage of Pratt and Whitney for providing the alloys used in this investigation.

References

1. G. R. BOOKER and J. NORBURY, *J. Appl. Phys.* **10** (1959) 543.
2. S. CARABAJAR, J. MERLIN, V. MASSARDIER and S. CHABANET, *Mater. Sci. Eng.* **A 281** (2000) 132.
3. S. E. KISAKUREK, *Metallography* **19** (1986) 19.
4. M. HILLERT, *Acta Metall.* **36** (1998) 3177.
5. R. A. STEVENS and P. E. J. FLEWITT, *Metallography* **11** (1978) 475.
6. A. M. WUSATOWSKA-SARNEK, M. J. BLACKBURN and M. AINDOW, *Mater. Sci. Eng.* **A 360** (2003) 390.
7. C. ZENER, *Trans. Metall. Soc. A. I. M. E.* **175** (1948) 15.
8. C. H. WÖRNER and P. M. HAZZLEDINE, *Scripta Metall. Mater.* **28** (1992) 337.
9. N. LOUAT, *Acta Metall.* **30** (1982) 1291.

Received 27 October 2004
and accepted 12 January 2005